Journal of Hazardous Materials 211–212 (2012) 218–225

Contents lists available at SciVerse ScienceDirect

Journal of Hazardous Materials

journal homepage: www.elsevier.com/locate/jhazmat

Photocatalytic activity of titanium dioxide nanoparticle coatings applied on autoclaved aerated concrete: Effect of weathering on coating physical characteristics and gaseous toluene removal

Anibal Maury-Ramirez [a], Kristof Demeestere [b,*], Nele De Belie [a]

[a] Magnel Laboratory for Concrete Research, Department of Structural Engineering, Faculty of Engineering and Architecture, Ghent University, Technologiepark Zwijnaarde 904, B-9052 Ghent, Belgium
[b] Research Group EnVOC, Department of Sustainable Organic Chemistry and Technology, Faculty of Bioscience Engineering, Ghent University, Coupure Links 653, B-9000 Ghent, Belgium

ARTICLE INFO

Article history:
Received 9 June 2011
Received in revised form 7 December 2011
Accepted 12 December 2011
Available online 21 December 2011

Keywords:
Titanium dioxide
Coating
Autoclaved aerated concrete
Weathering
Air purification

ABSTRACT

Autoclaved aerated concrete has been coated by TiO_2 nanoparticles through a dip-coating (DC) and a novel vacuum saturation (VS) method to investigate the weathering resistance and gaseous toluene removal potential of both coating types. The effect of intensive weathering – corresponding to a period of about 25 years – on the coating characteristics was studied in terms of TiO_2 content, coating thickness and color changes. Toluene removal was investigated in a lab-scale flow-through photoreactor at 24 °C and 52% relative humidity, and results obtained immediately after application of the coatings and after two weathering stages were compared. Weathering of the DC and VS coated samples resulted into a decrease of the coating layer thickness of more than 98%, confirmed by a decline in TiO_2 content by more than 99% and 93%, respectively. Surprisingly, toluene removal efficiencies before and after weathering kept constant at about 95% for both coating types, corresponding to an elimination rate of 60–70 mg/(m^2 h) at an initial toluene concentration of 15 ppm_v and a gas residence time of 3 min. Increasing the toluene load by applying higher toluene inlet concentrations (up to 35 ppm_v) and lower gas residence times (1 min) did decrease the toluene removal efficiency to 32–41%, but elimination rates increased up to 214 mg/(m^2 h), being a factor of 1.6–4.5 times higher than reported in recent work.

1. Introduction

Among other functional characteristics such as self-cleaning and anti-microbial properties, the application of titanium dioxide (TiO_2) photocatalysis on cementitious materials has also shown promising results as a novel technology to minimize air pollution in urbanized areas [1–4]. TiO_2 loaded materials have enabled the degradation of a range of organic (e.g. volatile organic compounds) and inorganic pollutants (e.g. NO_x and SO_2). Some pilot projects such as roads, parking lots, tunnels and other structures have been already constructed in different countries [5–7]. Technical aspects, however, still limit the large scale application and therefore the price of this light-driven technology. For example, it is not clear yet what is the most efficient way to incorporate the TiO_2 photocatalyst in the cementitious materials. Current research is conducted to minimize the amount of TiO_2 while enhancing the photocatalytic activity for the different applications.

Particularly towards air purification, Hüsken et al. [8] found that the roughness of the TiO_2 loaded material favored NO_2 and NO degradation using photocatalytic concrete. Similarly, Poon et al. [9,10] observed that incorporating recycled glass cullets into cementitious paving blocks raised the photocatalytic activity towards NO degradation. This was explained by porosity and light transmittance effects. Strini et al. [11,12] used a TiO_2 nanopowder embedded in white Portland cement to investigate the photocatalytic degradation of a gas mixture of benzene, toluene, ethylbenzene and o-xylene (BTEX). The highest photocatalytic activity was observed for o-xylene (elimination rate ER = 2.0 μmol/(m^2 h) ≈ 212.3 μg/(m^2 h)), followed by ethylbenzene > toluene > benzene. Instead of TiO_2 bulk mixing, Maury Ramirez et al. [4] tested different coating technologies on a number of concrete types in relation to their potential to remove toluene from air. Results indicated that concrete porosity was affecting positively the pollutant removal. In the best case, a TiO_2 dip-coating method applied on autoclaved aerated concrete samples was able to remove more than 85% toluene from air, corresponding to an ER of 48 mg/(m^2 h). In a similar approach, Demeestere et al. [1] investigated the photocatalytic activity of TiO_2 containing roofing tiles and corrugated sheets towards toluene degradation.

* Corresponding author at: Research Group EnVOC, Ghent University, Coupure Links 653, B-9000 Ghent, Belgium. Tel.: +32 9 264 59 65; fax: +32 9 264 62 43.
E-mail address: kristof.demeestere@ugent.be (K. Demeestere).

0304-3894/$ – see front matter © 2011 Elsevier B.V. All rights reserved.
doi:10.1016/j.jhazmat.2011.12.037

Through a detailed parameter study, removal efficiencies between 5 and 61% and ER between 67 and 107 mg/(m^2 h) were obtained, being to the best of our knowledge the highest toluene elimination rate on photocatalytic cementitious materials reported so far.

Although these are important achievements, a more detailed evaluation of the air purification potential of TiO_2 loaded cementitious materials during their entire design service life period is indispensable information for further technological development and sustainable full-scale application. So far, this information is scarce. However, the importance of material characteristics during extended periods of operation has been illustrated by a reduced photocatalytic activity due to cement carbonation [13], pore structure change during cement hydration [10], or by the presence of ionic species that contribute to charge recombination [14]. Particularly with respect to the durability and resistance to wear and/or weathering of photocatalytic coatings on cementitious materials, the available information is very limited [15,16]. Towards the effects of abrasive conditions on photocatalytic materials developed for air purifying purposes, only a scarcity of data focusing specifically on NO_x removal is reported. Yu [17] investigated the performance of concrete blocks containing TiO_2 in the upper layer by exposing them to real weathering in five different street locations (sidewalks) in the city of Hong Kong. After 4 months of exposure, the NO_x removal efficiency dropped by 36% to 78%. Hassan et al. [16] used a lab-scale instead of an in situ approach to evaluate the effect of accelerated traffic wearing on TiO_2 coated paving blocks and observed no significant effect on airborne NO removal. Data on weathering effects on the photocatalytic activity of vertically applied building envelope materials towards the removal of airborne organic pollutants, however, are lacking in open literature.

In this context, this paper presents new data in the field of photocatalytic research on cementitious materials intended for urban air purification, particularly towards the removal of volatile organic compounds. Using an accelerated test set-up – simulating a weathering period of about 25 years – the effects of intensive weathering on TiO_2 coatings applied on autoclaved aerated concrete are systematically investigated. Two different coating techniques have been studied: dip-coating and a novel vacuum saturation method. Both the physical characteristics like the TiO_2 content, coating thickness and color, and the photocatalytic performance towards gaseous toluene degradation at changing conditions of pollutant concentration and air flow are studied before and after weathering using the same set-up. This type of research is of crucial importance to better assess the real application potential of innovative cementitious materials for long-term air-purifying purposes.

2. Materials and methods

2.1. Materials

Autoclaved aerated concrete samples (AAC) were provided by Xella and cut into pieces with the following dimensions (length × width × height): 100 mm × 80 mm × 10 mm. The open porosity and roughness (Ra), determined by respectively vacuum saturation (ASTM C1202 Vacuum Saturation Method) and distance measurements using the automated laser measurement system (ALM) developed by De Belie et al. [18], of this material amount 74.9 ± 2.9% and 70 ± 27 μm, respectively [4].

Prior to the application of the dip-coating (DC) method, a set of 3 AAC samples was washed and dried in an oven (Vötsch – Industrietechnik) at 105 °C during 48 h. After cooling the samples inside a desiccator container, they were dipped during 5 min in a suspension of ethanol and TiO_2 (0.05 g/mL) that had been previously stirred during 30 min. Next, the samples were dried at 105 °C during 48 h. Based on this DC technique, a new vacuum saturation (VS) coating method has been developed. In this case, after the 3 AAC samples were washed and dried, they were installed in a vacuum saturation tank at 100 mbar during 2.5 h. Afterwards, the TiO_2-ethanol suspension (0.05 g/mL) was injected into the vacuum tank to coat the samples. When all samples were covered with the suspension, the vacuum process was stopped and the samples were left in the open vacuum tank during at least 30 min, prior to drying at 105 °C during 48 h. For comparison, also a set of 3 uncoated AAC samples (REF) was evaluated during the experiments.

Both DC and VS coatings were applied using TiO_2 nanoparticles from the same origin (ANX Type N100). This is an experimental nanocrystalline TiO_2 obtained from Kemira Pigments Oy (Pori, Finland). An X-ray diffractometric analysis with a step size of 0.02 degrees and a step time of 1 s (Siemens D5000) on this TiO_2 showed a pure anatase composition, with a specific surface area of 100 m^2/g as determined by volumetric N_2-gas adsorption (Belsorp-mini II). Information supplied by the manufacturer indicates a crystal size of 20 nm (TEM microscope) and a particle size (d_{50}) of 2 μm (laser diffraction). Additionally, according to the manufacturer, the content of sulphur (0.4%; ICP-AES), Fe_2O_3 (70 mg/kg; X-ray fluorescence) and sodium (150 mg/kg; AAS) makes this TiO_2 ideal for photoactive concrete due to its low alkali metal and sulphur contents.

2.2. Accelerated weathering process

The weathering process applied on the coated concrete samples was investigated in a laboratory accelerated weathering test set-up that simulates in a fast way a typical facade abrasion process. By creating every 12 h rain-day and dry-night coordinated cycles, the samples were weathered during 2 consecutive stages (WI and WII) lasting 7 days each. Considering the simulated rain conditions (120 mm/h) applied in the test set-up on the one hand, and the Belgium average cumulative precipitation index (800 mm/year) on the other hand, the total weathering process (WI and WII) represents approximately 25 years of weathering. Operating in a different mode, this test set-up has been previously used by De Muynck et al. [19] and Maury-Ramirez and De Belie [2] to evaluate algae growth on cementitious materials treated with water repellents, biocides or photocatalytic particles. The test set-up consists of inclined (45°) PVC (polyvinyl chloride) compartments in which samples are placed. The rain condition is produced in each compartment by pumping 1 L of mineral water during 12 h by means of a NW33 aquarium pump. Since rain water is not circulating in real circumstances, the mineral water is replaced after 3.5 days in each compartment to obtain a better similarity with real rain conditions. Dry conditions are obtained by switching off the pumps during 12 h. Day and night conditions are respectively coordinated with the rain and dry conditions and last also 12 h each one. A day condition is created by means of several Grolux 30 W lamps (light spectrum with peaks around 365, 400, 440, 550 and 580 nm). The illumination level was 800 ± 84 lux, 524 ± 62 lux, and 448 ± 114 lux at the upper, middle and lower parts of the PVC compartments, respectively. Similarly, night condition is obtained by switching off the lamp system. The test set-up is placed in an air-conditioned room in which the changes in temperature and relative humidity (RH) during the cycles are monitored using a thermo-hygrometer Logger Testo 175 – H2. During the weathering process, RH amounted 90 ± 4% and 94 ± 3% during day and night cycles, respectively. Temperatures reached 22 ± 1 °C and 20 ± 1 °C also during day and night cycles, respectively. In order to have more representativeness of this test, 3 sample repetitions from each coating type were used.

2.3. Physical characterization of the coatings

For evaluating the effect of the weathering process on the coated samples, 3 different physical parameters were determined just after coating application (W0) and after the first and second weathering stages (WI and WII). First, the TiO_2 content of the coated and weathered samples was determined as the difference in mass between the non-coated samples and the coated samples at stage W0, WI, and WII. An analytical balance (Mettler Toledo AG04) with a precision of 0.1 mg was used. Prior to all mass measurements, the concrete samples were oven (Vötsch – Industrietechnik) dried at 105 °C, after which they were cooled down in a desiccator container during 30 min. Secondly, in order to visualize the coating morphology changes and especially the thickness evolution because of weathering, coated samples were cut in suitable sizes (less than 1 cm^3 approx.), and Scanning Electron Microscopy (SEM) equipped with Energy-dispersive X-ray spectroscopy (EDAX) analysis (Philips XL 30 ESEM) was performed before and after weathering. The coating thickness (t) was then determined (when possible) by using a graphical measurement tool of the software (supplied by SEM producer) on at least 10 different points randomly distributed on each coated sample. Finally, color changes (ΔE_i) produced by the weathering stages were measured by a Colorimeter (X-rite SP60) with an 8 mm aperture and calculated based on the CIE Lab color system as indicated in Eq. (1). In order to evaluate the coating removal, color changes produced by a weathering stage (ΔE_i) were always based on a comparison between the color measurements after coating and weathering (L_i, a_i, b_i) and before coating application (L_0, a_0, b_0). On each coated sample, color measurements were done at 3 different fixed positions.

$$\text{Color change,} \quad \Delta E_i = \sqrt{\Delta L_i^2 + \Delta a_i^2 + \Delta b_i^2} \tag{1}$$

with $\Delta L_i = L_i - L_0$; $\Delta a_i = a_i - a_0$; $\Delta b_i = b_i - b_0$.

2.4. Air purification experiments

The photocatalytic air purification potential of the TiO_2 coated autoclaved aerated concrete was studied towards gaseous toluene (TOL) removal in a lab-scale rectangular flat-plate plexiglass flow-through reactor (length (L): 20 cm; width (W): 10 cm; height (H): 4 cm). Toluene was selected as a model pollutant given its relevance in ambient air pollution as reported by different research groups worldwide [20–22]. UV irradiation was provided by a black-light blue 18 W UV lamp ($340 < \lambda\ (nm) < 410$; maximum emission at 365 nm, Philips Lighting, Turnhout, Belgium), covered by a half cylindrical reflector and positioned just above the 2.2 mm thick borofloat glass-plate closing the reactor. Using potassium ferrioxalate actinometry, light intensity (I) at the catalyst surface was determined to be 2.3 mW/cm^2, being of the same order of magnitude as can be expected during sunny days in Central Europe [8]. TOL inlet concentrations and gas residence times (τ) were controlled at given values between 15 and 35 ppm_v and between 1 and 3 min, respectively. Because of the sensitivity limits of the analytical method used [23], the toluene concentration level was put at the low ppm_v range instead of the ambient ppb_v levels. These higher concentration levels allow a mutual comparison of the DC and VS coating activity when exposed at rather severe conditions in terms of pollutant level. The applied gas residence time, which is a factor of 3–20 shorter than that in the work of Strini et al. [11] and Chen et al. [24], allowed a fair comparison of our data with those obtained with other types of cementitious materials studied in the same set-up [4]. The RH of the TOL-loaded air stream and the temperature within the reactor were registered at $51.8 \pm 0.1\%$ and 23.7 ± 0.2 °C during all experiments by means of a TESTO 110 sensor device (TESTO NV). These values are similar to those valid in ambient environment. Gas sampling points were provided at both the inlet and outlet of the reactor. Inlet and outlet air samples were taken by solid-phase microextraction (SPME) using a 100 μm polydimethylsiloxane fibre (Supelco) as the extraction phase. Chemical analyses were carried out on an Agilent 6890 Series gas chromatograph, equipped with a flame ionization detector (FID, 250 °C) fed by 400 mL/min air and 40 mL/min hydrogen. The carrier gas was helium with a flow rate of 3 mL/min. A SPME inlet liner was installed and placed at a temperature of 200 °C. Separation was done on a 30 m × 0.53 mm cross linked methylsiloxane capillary column with a film thickness of 5.0 μm (HP-1, Santa Clara). Equilibrated water–gas systems with a known toluene headspace concentration were used for calibration [25].

Prior to all photocatalytic degradation experiments, humidified TOL contaminated air was passed through the reactor in the absence of UV irradiation for at least 12 h to obtain the desired RH and TOL gas–solid adsorption–desorption equilibrium throughout the whole reactor. The latter was exemplified by TOL in- and outlet concentrations not significantly different from each other (t-test, significance level $\alpha \geq 0.05$). This 12 h period is significantly longer than that suggested (1.5 h) in the Japanese standard JIS R 1701-3:2008, which reports a test method for evaluating the air purification performance of fine ceramic photocatalytic materials particularly towards toluene removal [26]. Due to the high porosity of the autoclaved aerated concrete, however, the adsorption equilibrium time on this material might be longer. Therefore, and for practical reasons, equilibration was done overnight. Afterwards, the UV lamp was switched on and photocatalytic TOL degradation was carefully followed for at least 30 h, being 10 times longer than advised in the Japanese standard test (JIS R 1701-3:2008). Since deactivation of the catalyst surface may occur during the treatment of BTEX loaded waste gases [27–29], this extended irradiation time was selected in order to evaluate the stability of the photocatalytic cementitious materials towards toluene degradation. Finally, the lamp was switched off and the TOL in- and outlet concentrations were measured for an additional period of approximately 12 h. The TOL removal efficiency ($\eta_{removal}$), loading (LR) and elimination (ER) rates are calculated as presented in Eqs. (2)–(4). Here, Q (L/h) is the total air flow passing through the photoreactor, A (m^2) represents the geometric area of the TiO_2 coated concrete sample exposed to TOL-loaded gas and light, and $[TOL]_{in}$ and $[TOL]_{out}$ are the toluene concentrations (mg/L) at the reactor inlet and outlet, respectively. All these parameters are calculated with all obtained data from the UV-irradiated periods using 2 sample repetitions for each coating type.

$$\eta_{removal}\ (\%) = \left(1 - \frac{[TOL]_{out}}{[TOL]_{in}}\right) \times 100 \tag{2}$$

$$LR\ \ (mg\ \ TOL/(m^2\ h)) = \frac{Q}{A} \times [TOL]_{in} \tag{3}$$

$$ER\ \ (mg\ \ TOL/(m^2\ h)) = \frac{Q}{A} \times ([TOL]_{in} - [TOL]_{out}) \tag{4}$$

3. Results and discussion

3.1. Effect of weathering on the physical coating characteristics

The evolution of the TiO_2 content, coating thickness and color changes monitored before (W0) and after weathering (WI and WII) of the coated samples (DC and VS) is shown in Fig. 1. Before weathering, a clear difference in the physical parameters of both types of coatings is observed. The estimated TiO_2 content on the VS samples (11.1 ± 0.9 g) compared to the TiO_2 content of DC samples (2.3 ± 0.4 g) is almost five times larger. For the latter coatings, the amount of TiO_2 is similar to that embedded in an autoclaved aerated concrete block (density: 0.65 g/cm^3) having the same dimensions

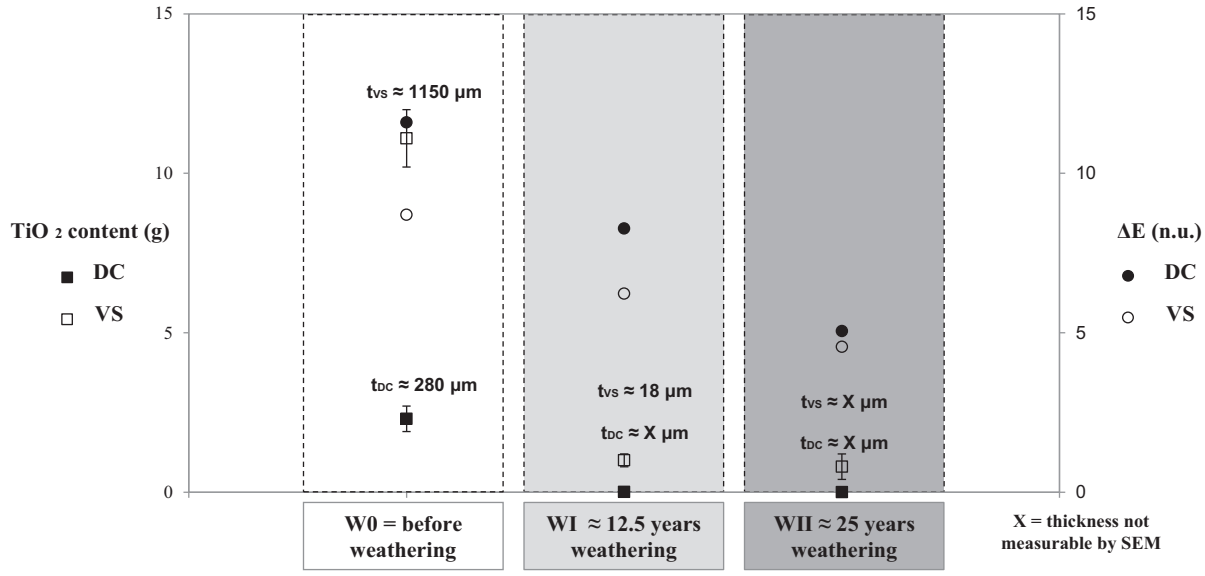

Fig. 1. TiO_2 content (g), coating thickness (t_{DC}/t_{VS}, μm) and color changes (ΔE_i, no units) before (W0) and after the weathering stages (WI and WII) on DC and VS coated samples.

as used in this study and containing 5% of TiO_2 mixed in its bulk material. However, in the case of coatings, all TiO_2 is present at the outer surface of the concrete material which is less susceptible to blocking phenomena caused by e.g. cement hydration products [24] than TiO_2 nanoparticles embedded in a cement matrix. Thus, TiO_2 in coatings is expected to be more accessible to both pollutant molecules and light photons. The coating thickness measured on VS samples (t_{VS} = 1150 μm) showed to be four times larger than that on DC samples (t_{DC} = 280 μm). Differences between both coating types are less pronounced with respect to color changes compared to the original substrate color. The color change on DC samples (ΔE = 11.6) was slightly more pronounced than that taking place on the VS samples (ΔE = 8.7). The produced color changes were mainly due to the whiter color (reflected by L values) from the TiO_2 particles compared to the AAC substrate, and also due to the development of light yellow stains (reflected by a values) after the coated samples were dried in the oven.

After the first and second weathering stage, the TiO_2 content significantly decreased in both coated sample types. In the VS samples, the TiO_2 content dropped by 90% and 93% after WI and WII, respectively, while no significant difference was measured between the mass of weathered DC samples and non-coated samples. Similarly, the coating thickness of the VS samples dropped from 1150 to 18 μm (98% reduction) after WI, corresponding well with the decrease in TiO_2 content. The coating thickness of the VS samples after WII and of weathered DC samples (after both WI and WII) was no longer measurable. Color changes induced by the weathering stages (WI and WII) were similar for both coating types, i.e. ΔE values reached 5.0 and 4.6 for DC and VS, respectively.

The changes in morphology of the coatings DC and VS before (W0) and after weathering (WI and WII) can also be observed from the SEM pictures presented in Figs. 2 and 3. The morphology of both coating types before the application of any weathering (W0) is shown at a 100× magnification in both top (Figs. 2a and 3a) and cross section (Figs. 2b and 3b) views. The DC coating is a thin flat layer characterized by the presence of cracks and pores (Fig. 2a), while the VS coating shows a more homogeneous surface without defects (Fig. 3a). After the first weathering (WI), the cross sectional SEM picture reveals a clearly reduced TiO_2 layer thickness on the VS sample (Fig. 3d, 4000× magnification), while no distinct layer could be observed on the DC sample (not shown). This effect was even stronger after the second weathering since no layer was visible on both types of coatings in the cross section view, even at a magnification of 8000×. The disappearance or less pronounced presence of the coating layer after weathering is confirmed when looking at the top view pictures after WI and WII. For example, when comparing Fig. 2a with 2c (DC) and Fig. 3a with 3c (VS), a much rougher surface is observed after weathering of both sample types. The observed roughness can be attributed to the AAC substrate material which is no longer covered by a thick dense TiO_2 layer.

3.2. Effect of weathering on photocatalytic toluene removal from air

As an illustration of a typical experiment, Fig. 4a shows the TOL inlet and outlet concentrations measured as a function of time during dark (no UV-irradiated) and UV-irradiated periods using a VS sample. Both before and after weathering stage WI and WII, highly reproducible toluene removal efficiencies of about 95% were obtained during UV-irradiation at a TOL inlet concentration of 15 ppm_v and a 3 min gas residence time. In contrast, no significant difference between TOL in- and outlet concentrations is measured in the dark. In a similar experiment, toluene removal on a non-coated AAC sample (REF) was investigated at the same conditions of inlet concentration, gas residence time, RH, and temperature. Fig. 4b clearly shows that no significant toluene removal is obtained with this REF sample, as exemplified by toluene inlet and outlet concentrations of 12.0 ± 0.5 and 12.6 ± 0.2 ppm_v, respectively, during UV irradiation.

Both type of coatings (DC and VS) were evaluated in duplicate according to the procedure as depicted in Fig. 4a. Table 1 summarizes the experimental conditions and results obtained both before and after the accelerated weathering stages (I and II). It can be noticed that although both coating types have different physical characteristics (see Section 3.1), their behaviour towards photocatalytic toluene removal is highly similar, with removal efficiencies as high as 93–95% independent of the degree of weathering. Considering the significant reduction of the TiO_2 content and layer thickness in both DC and VS coatings during the whole weathering process (see Section 3.1), this result is at least surprising. SEM-EDAX analysis revealed, however, the presence

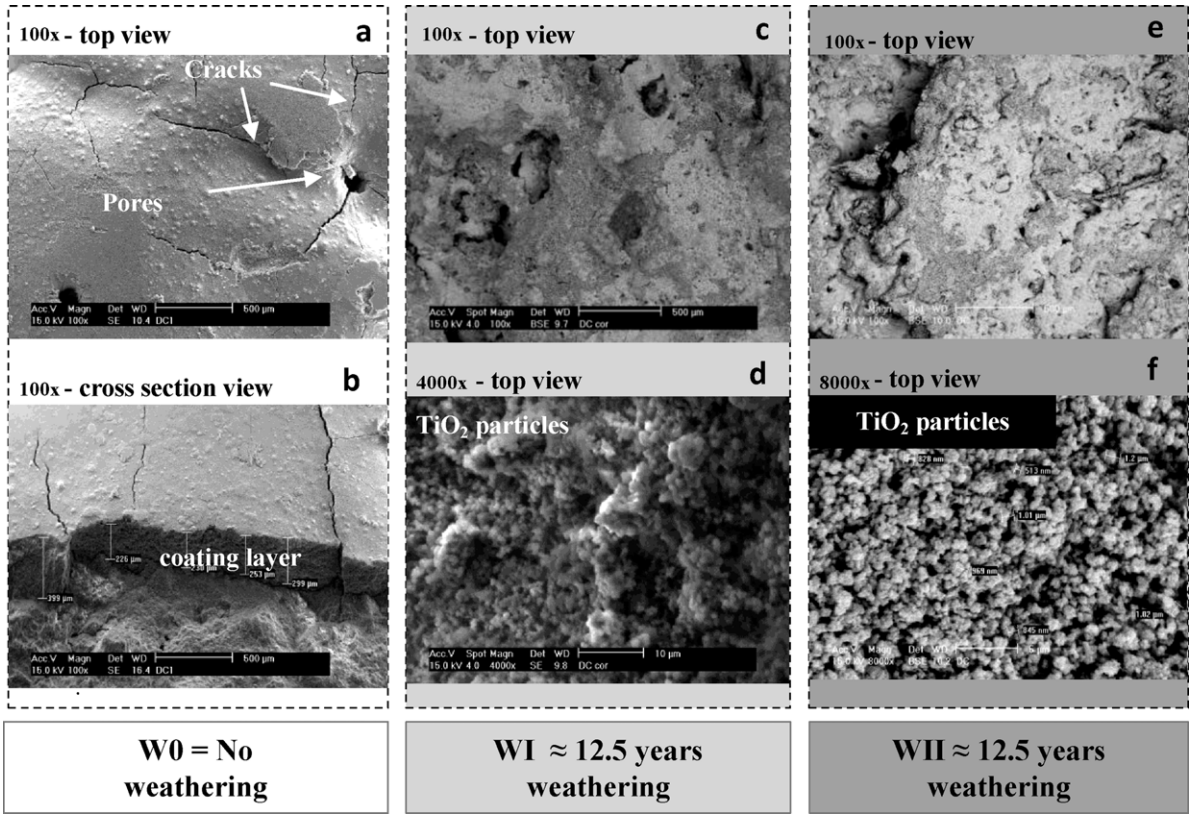

Fig. 2. SEM pictures of the DC coating appearance before (W0) and after weathering (WI and WII).

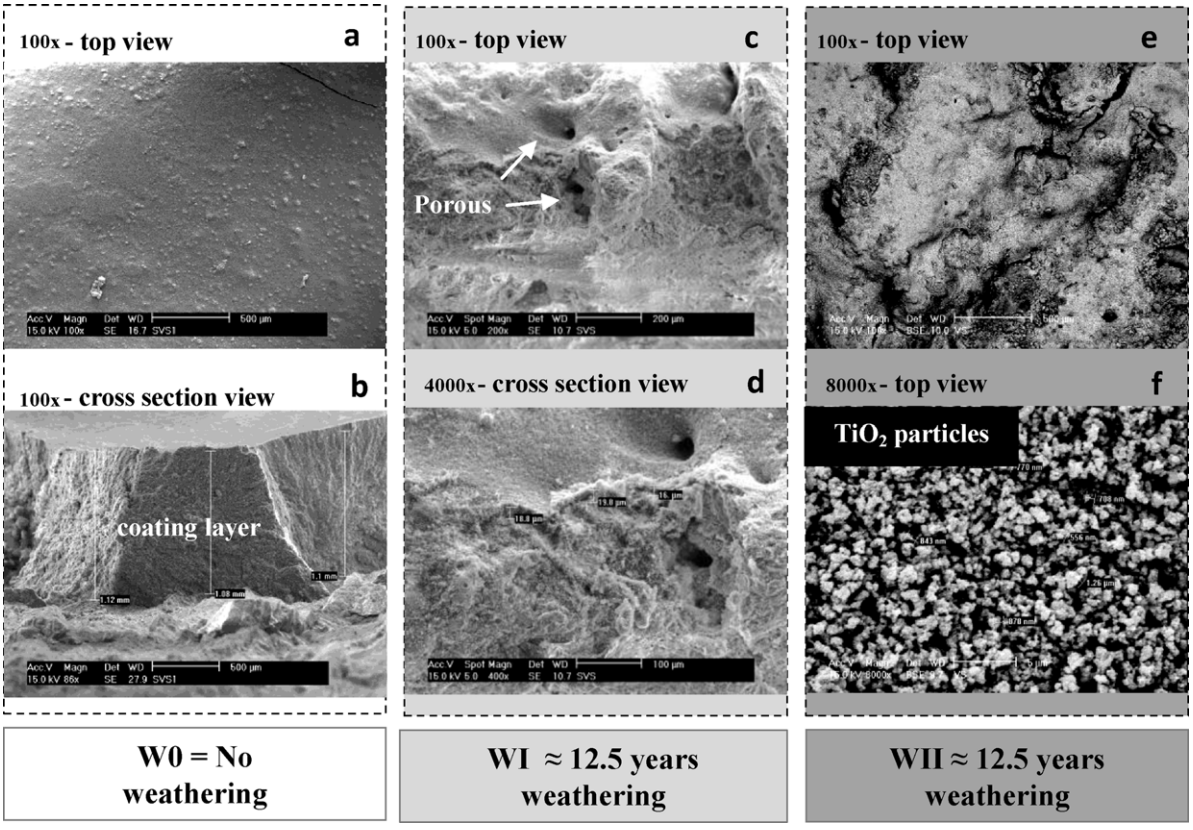

Fig. 3. SEM pictures of the VS coating appearance before (W0) and after weathering (WI and WII).

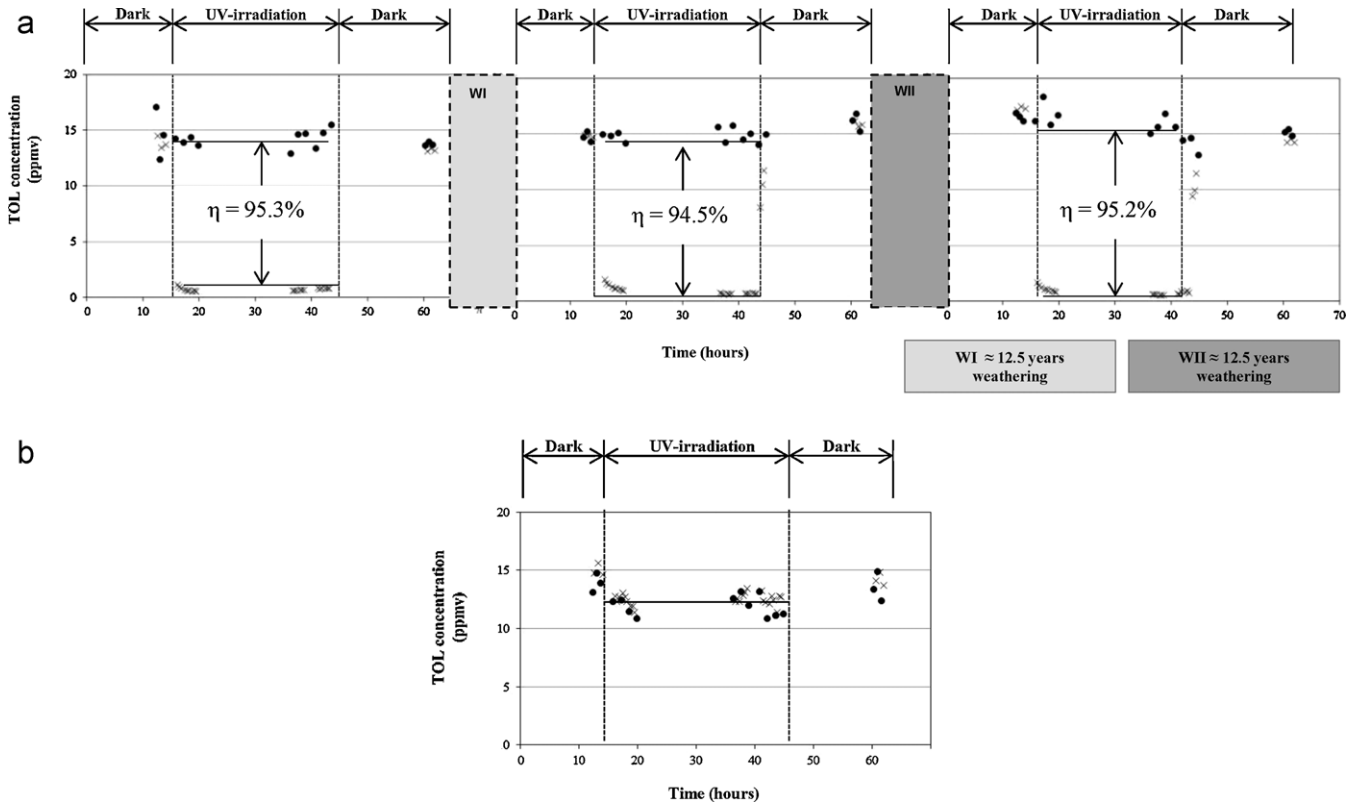

Fig. 4. (a) Gas phase TOL inlet (●) and outlet (×) concentrations during an air purification experiment using a concrete sample coated by vacuum saturation (VS); η (%): removal efficiency. (b) Gas phase TOL inlet (●) and outlet (×) concentrations during an air purification experiment using an uncoated concrete sample (REF).

of heterogeneously distributed TiO_2 nanoparticles still present at the substrate surface even after the second weathering stage. The heterogeneity of the surface is clear in Figs. 2e and 3e showing alternating lighter and darker regions as a result of changing TiO_2 content as supported by EDAX analyses at different spots (results not included). Therefore, our findings indicate that the remaining TiO_2 nanoparticles result in a preserved photocatalytic activity at the studied conditions of pollutant concentration, residence time, temperature, RH and UV-irradiation intensity. This might open interesting perspectives for further optimization of TiO_2 coating developments in terms of minimization of the needed TiO_2 content and enhancing the efficiency of the catalyst use.

In order to subject both type of coatings to higher toluene loading rates (LR), both the gas flow rate and the inlet concentration were varied. Consequently, the toluene removal on the weathered DC and VS coated AAC samples (i.e. after WII) was measured at inlet concentrations up to 35 ppm_v and gas residence times between 1 and 3 min, corresponding to loading rates between 65 and 540 mg/(m^2 h). Results are given in Fig. 5. By reducing the residence time by a factor of 3, the toluene removal efficiency dropped from about 95% ($[TOL]_{in}$ = 15 ppm_v and τ = 3 min) to about 50% for both coatings (TOL_{in} = 15 ppm_v and τ = 1 min). Similarly, increasing the inlet concentration by a factor of 2 ($[TOL]_{in}$ = 35 ppm_v and τ = 1 min) further decreased the toluene removal efficiency to 41% and 32% for DC and VS coated samples, respectively. Despite this decline in removal efficiency, the TOL elimination rates (ER) increased from 60–70 mg/(m^2 h) to 166–214 mg/(m^2 h) at increasing loading rate. In the same test set-up and at similar conditions (12 ppm_v toluene inlet concentration; RH = 41%; T = 25 °C; τ = 3 min, I = 2.3 mW/cm^2), Maury Ramirez et al. [4] obtained toluene removal efficiencies

Table 1
Average and standard deviation (SD) of the toluene inlet concentrations ($[TOL]_{in}$, ppm_v), removal efficiencies ($\eta_{removal}$, %), relative humidity (RH, %) and temperatures (T, °C) measured for the DC and VS coatings (n = 2) during 30 h of UV-irradiation before (W0) and after weathering (WI and WII).

Sample condition	Parameter	Dip-coating (DC)		Vacuum saturation (VS)	
		Average	SD	Average	SD
Before weathering (W0) = initial condition	$[TOL]_{in}$ (ppm_v)	14.9	0.4	14.3	0.1
	$\eta_{removal}$ (%)	93.2	2.1	95.1	0.3
	RH (%)	56.5	0.5	49.8	9.1
	T (°C)	24.3	0.6	25.3	0.6
After first weathering (WI) = 12.5 years of weathering	$[TOL]_{in}$ (ppm_v)	14.8	0.1	12.5	3.3
	$\eta_{removal}$ (%)	95.4	0.5	94.8	0.4
	RH (%)	51.3	0.4	50.7	0.1
	T (°C)	22.8	0.4	22.8	0.5
After second weathering (WII) = 12.5 years of weathering	$[TOL]_{in}$ (ppm_v)	13.3	0.0	15.5	0.4
	$\eta_{removal}$ (%)	93.7	1.3	95.1	0.2
	RH (%)	52.9	5.2	48.5	0.8
	T (°C)	22.5	0.5	21.8	0.1

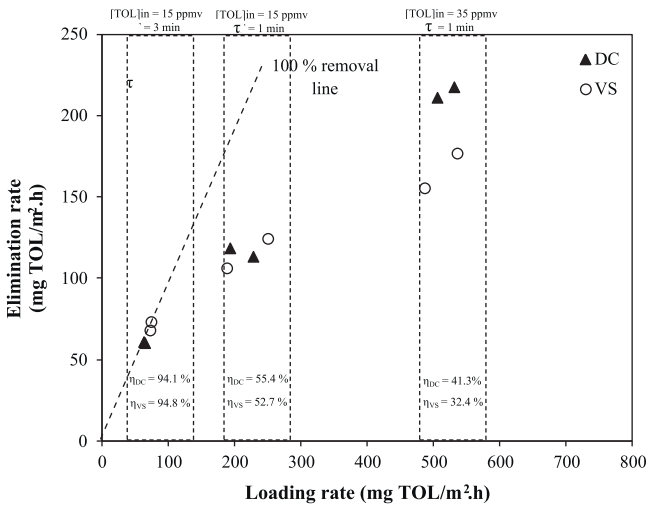

Fig. 5. Elimination rates (ER), loading rates (LR) and toluene removal efficiencies ($\eta_{removal}$) at different gas residence times (τ = 1 to 3 min) and toluene inlet concentrations ($[TOL]_{in}$ = 15 to 35 ppm_v) using DC and VS samples.

from 41% to 86% (equivalent to ER from 28 to 48 mg/(m^2 h)) using different dip-coated concrete types. When using a sol–gel method on the same concrete types, however, removal efficiencies did not exceed 4% (corresponding to a maximum toluene ER of 4.0 mg/(m^2 h)). Using TiO_2 containing roofing tiles and corrugated sheets, Demeestere et al. [1] obtained toluene removal efficiencies and ER up to 61% and 107 mg/(m^2 h), respectively, at toluene inlet concentrations between 23 and 465 ppm_v, RH = 50%, T = 25 °C, τ = 2 min and I = 2.3 mW/cm^2. Other researchers like Strini et al. [11] used TiO_2 nanopowder embedded in white Portland cement to degrade BTEX compounds from air at concentrations of 400 μg/m^3, RH = 50%, T = 23 °C, τ = 20 min and I = 1.36 mW/cm^2. Removal efficiencies between 5% and 54% were obtained, corresponding to ER up to 120 μg/(m^2 h). Contrary, Chen et al. [24] evidenced no toluene removal at different inlet concentrations (200–800 ppb), neither as a single compound nor when mixing toluene with NO (400 ppb), using TiO_2 added concretes (5% and 10% on a weight basis). In this case, temperature, relative humidity, gas residence time and light intensity amounted to 25 °C, 50%, 1.5–9.0 min, and 1 mW/cm^2, respectively.

The observed relationship between ER and LR (Fig. 5) is in agreement with other studies [1,3,11] and illustrates the importance of both mass transfer effects and chemical reaction kinetics on the TiO_2 nanoparticles surface in the overall toluene removal rate [27]. It is clear that the highest ER are obtained for the DC concrete sample, although this type of coating was more susceptible to weathering in terms of coating thickness and TiO_2 content. One possible explanation might be that TiO_2 nanoparticles in the VS sampled are located more deeply in the substrate because of the applied vacuum during coating. This may result into a lower accessibility of the nanoparticles towards both toluene molecules and photons. It should be stressed, however, that the DC as well as the VS coatings show very promising air purification potential compared to recent literature data. For example, the toluene elimination rates obtained in this research are – even after 25 years of weathering – a factor of 1.6 to 4.5 higher than those reported in other recent work dealing with the removal of toluene on TiO_2 coated ceramic tiles and concrete [1,4]. Although the results of this paper indicate a benefit for the technical less complicated DC technique compared to the VS method from the purpose of air purification, further research is needed to fully compare the advantages and limitations of both coating techniques. Hereby, an in situ validation exposing the materials to mixtures of pollutants (both other organic and inorganic contaminants like the traffic-related NO_x) at real conditions and ambient concentration levels might be useful, and also the study of other photocatalytic applications like e.g. self-cleaning and anti-algal fouling effects should be of added value. Attention should be paid in further research to the carbon mineralization efficiency of organic contaminants and to the formation of possible intermediate products. Next to that, a life cycle assessment (LCA) of both types of TiO_2 coated autoclaved aerated concrete could be helpful to take into account both the energy and resource inputs for their production and utilization phase and the possible effects of TiO_2 release into the environment as a result of weathering.

4. Conclusions

This paper brings forward new data on intensive weathering effects on TiO_2 coated cementitious materials. Although the durability of this kind of materials was hardly investigated so far, the lack of knowledge on this issue has been identified as one of the main obstacles for large-scale implementation of heterogeneous photocatalysis in the construction sector. For the first time, this work focuses on both the physical and photocatalytic properties of autoclaved aerated concrete, commonly used as vertical wall partition elements, before and after weathering. Coating with TiO_2 was done using two different techniques: dip-coating (DC) and a new vacuum saturation (VS) method. Two main conclusions can be drawn. First, both types of coatings show high air purification potential towards toluene removal, as exemplified by removal efficiencies higher than 95% and elimination rates up to 75 mg/(m^2 h). Second, accelerated and intensive weathering, simulating a period of 25 years at central Europe weather conditions, clearly affected the physical characteristics of the coatings, as exemplified by a significant decrease in both the TiO_2 mass and the coating thickness by 93–99% and more than 98%, respectively. Nevertheless, and quite surprisingly, their photocatalytic activity towards toluene removal was maintained. Applying shorter gas residence times and higher toluene concentrations did even increase the toluene elimination rates up to 214 mg/(m^2 h), although removal efficiencies decreased to 32–41%. Our results strongly indicate that the heterogeneously distributed TiO_2 nanoparticles present at the substrate surface after weathering – as confirmed by SEM-EDAX – still act as the active sites preserving photocatalytic activity on the autoclaved aerated concrete sample.

Acknowledgements

The authors would like to thank the funding given by Ghent University via the BOF grant 01W04308. We are also grateful to Ghent University personnel who supported us in many different tests. Specially, Dr. Ir. Willem De Muynck and Ir. Christophe Walgraeve for their collaboration in the design and construction of the weathering and air-purification test set-ups, respectively. Similarly, the kind supply of TiO_2 for these experiments done by Kemira Chemicals is acknowledged.

References

[1] K. Demeestere, J. Dewulf, B. De Witte, A. Beeldens, H. Van Langenhove, Heterogeneous photocatalytic removal of toluene from air on building materials enriched with TiO_2, Build. Environ. 43 (2008) 406–414.
[2] A. Maury Ramirez, N. De Belie, Evaluation of the algaecide activity of titanium dioxide on autoclaved aerated concrete, J. Adv. Oxid. Technol. 12 (2009) 100–104.
[3] A. Maury, N. De Belie, State of the art of TiO_2 containing cementitious materials: self-cleaning approach, Mater. Constr. 60 (2010) 33–50.
[4] A. Maury Ramirez, K. Demeestere, N. De Belie, T. Mäntylä, E. Levänen, Titanium dioxide coated cementitious materials for air purifying purposes: preparation, characterization and toluene removal potential, Build. Environ. 45 (2010) 832–838.

[5] G. Guerrini, E. Peccati, Photocatalytic cementitious roads for depollution, in: P. Baglioni, L. Cassar (Eds.), Proceedings of the International RILEM Symposium on Photocatalysis, Environment and Construction Materials, RILEM Publications SARL, Florence, Italy, 2007, pp. 179–186.
[6] A. Beeldens, Air purification by road materials: results of the test project in Antwerp, in: P. Baglioni, L. Cassar (Eds.), Proceedings of the International RILEM Symposium on Photocatalysis, Environment and Construction Materials, RILEM Publications SARL, Florence, Italy, 2007, pp. 187–194.
[7] T. Maggos, J.G. Bartzis, M. Liakou, C. Gobin, Photocatalytic degradation of NO_x gases using TiO_2-containing paint: a real scale study, J. Hazard. Mater. 146 (2007) 668–673.
[8] G. Hüsken, M. Hunger, H.J.H. Brouwers, Experimental study of photocatalytic concrete products for air purification, Build. Environ. 44 (2009) 2463–2474.
[9] C.S. Poon, E. Cheung, NO removal efficiency of photocatalytic paving blocks prepared with recycled materials, Constr. Build. Mater. 21 (2007) 1746–1753.
[10] J. Chen, C.S. Poon, Photocatalytic activity of titanium dioxide modified concrete materials – influence of utilizing recycled glasscullets as aggregates, J. Environ. Manage. 90 (2009) 3436–3442.
[11] A. Strini, S. Cassese, L. Schiavi, Measurement of benzene, toluene, ethylbenzene and o-xylene gas phase photodegradation by titanium dioxide dispersed in cementitious materials using a mixed flow reactor, Appl. Catal. B 61 (2005) 90–97.
[12] A. Strini, L. Schiavi, Low irradiance toluene degradation activity of a cementitious photocatalytic material measured at constant pollutant concentration by a successive approximation method, Appl. Catal. B 103 (2011) 226–231.
[13] M. Lackhoff, X. Prieto, N. Nestle, F. Dehn, R. Niessner, Photocatalytic activity of semiconductor-modified cement-influence of semiconductor type and cement ageing, Appl. Catal. B 43 (2003) 205–216.
[14] A. Rachel, M. Subrahmanyam, P. Boule, Comparison of photocatalytic efficiencies of TiO_2 in suspended and immobilised form for the photocatalytic degradation of nitrobenzenesulfonic acids, Appl. Catal. B 37 (2002) 301–308.
[15] B. Daniotti, S. Lupica Spagnolo, R. Galliano, The durability experimental evaluation of photocatalytic cement-based materials, in: Proceedings of the International Conference on Durability of Building Materials and Components, Porto, Portugal, 2011, pp. 1–8.
[16] M.M. Hassan, H. Dylla, L.N. Mohammad, T. Rupnow, Evaluation of the durability of titanium dioxide photocatalyst coating for concrete pavement, Constr. Build. Mater. 24 (2010) 1456–1461.
[17] J.C.-M. Yu, Deactivation and regeneration of environmentally exposed titanium dioxide (TiO2) based products. Testing report prepared for the Environmental Protection Department HKSAR, Hong Kong, China, 2003, pp. 1–21.
[18] N. De Belie, J. Monteny, A. Beeldens, E. Vincke, D. Van Gemert, W. Verstraete, Experimental research and prediction of the effect of chemical and biogenic sulfuric acid on different types of commercially produced concrete sewer pipes, Cem. Concr. Res. 34 (2004) 2223–2226.
[19] W. De Muynck, A. Maury Ramirez, N. De Belie, W. Verstraete, Evaluation of strategies to prevent algal fouling on white architectural and cellular concrete, Int. Biodeter. Biodegrad. 63 (2009) 679–689.
[20] X. Han, L.P. Naeher, A review of traffic-related air pollution exposure assessment studies in the developing world, Environ. Int. 32 (2006) 106–120.
[21] R. Bono, E.H. Bugliosi, T. Schiliro, G. Gilli, The Lagrange street story: the prevention of aromatics pollution during the last nine years in a European city, Atmos. Environ. 35 (Suppl. 1) (2001) S107–S113.
[22] A.B. Hansen, F. Palmgren, VOC air pollutants in Copenhagen, Sci. Total Environ. 190 (1996) 451–457.
[23] J. Van Durme, K. Demeestere, J. Dewulf, F. Ronsse, L. Braeckman, J. Pieters, H. Van Langenhove, Accelerated solid-phase dynamic extraction of toluene from air, J. Chromatogr. A 1175 (2007) 145–153.
[24] J. Chen, S.C. Kou, C.S. Poon, Photocatalytic cement-based materials: comparison of nitrogen oxides and toluene removal potentials and evaluation of self-cleaning performance, Build. Environ. 46 (2011) 1827–1833.
[25] J. Van Durme, J. Dewulf, W. Sysmans, C. Leys, H. Van Langenhove, Efficient toluene abatement in indoor air by a plasma catalytic hybrid system, Appl. Catal. B 74 (2007) 161–169.
[26] Japanese Standards Association, JIS R 1701-3 Fine ceramics (advanced ceramics, advanced technical ceramics) – test method for air purification performance of photocatalytic materials – Part 3: Removal of toluene, Japanese Industrial Standard JIS (2008) 1–8.
[27] K. Demeestere, J. Dewulf, H. Van Langenhove, Heterogeneous photocatalysis as an advanced oxidation process for the abatement of chlorinated, monocyclic aromatic and sulfurous volatile organic compounds in air: state of the art, Crit. Rev. Environ. Sci. Technol. 37 (2007) 489–538.
[28] V. Augugliaro, S. Coluccia, V. Loddo, L. Marchese, G. Martra, L. Palmisano, M. Schiavello, Photocatalytic oxidation of gaseous toluene on anatase TiO_2 catalyst: mechanistic aspects and FT-IR investigation, Appl. Catal. B 20 (1999) 15–27.
[29] Y. Luo, D.F. Ollis, Heterogeneous photocatalytic oxidation of trichloroethylene and toluene mixtures in air: kinetic promotion and inhibition, time-dependent catalyst activity, J. Catal. 163 (1996) 1–11.